energy&fuels

Article

pubs.acs.org/EF

Asphaltene Grading and Tar Mats in Oil Reservoirs

Julian Y. Zuo,*[,†] Oliver C. Mullins,[‡] Vinay Mishra,[#] German Garcia,[⊥] Chengli Dong,[#] and Dan Zhang[†]

[†]DBR Technology Center, Schlumberger, Edmonton, AB T6N 1M9, Canada

[‡]Schlumberger Doll Research, One Hampshire Street, Cambridge, Massachusetts 02139, United States

[#]Schlumberger Oilfield Services, 1325 South Dairy Ashford, Houston, Texas 77077, United States

[⊥]Schlumberger OFS Servicios, Villahermosa, Tabasco, Mexico

ABSTRACT: Advances in asphaltene science and a new generation of downhole fluid analysis (DFA) technology have been combined to yield powerful new insights to reservoir tar mats. The asphaltene nanoscience model, the modified Yen model, also known as the Yen−Mullins model, has enabled development of the industry's first predictive equation of state for asphaltene concentration gradients. This equation of state (EOS) is a modified Flory−Huggins regular solution model for the asphaltene part that has been referred to as the Flory−Huggins−Zuo (FHZ) EOS for asphaltene concentration gradients in oil reservoirs. Measurement of these gradients using "downhole fluid analysis" coupled with analysis using the FHZ EOS has successfully addressed a variety of reservoir concerns including reservoir connectivity, viscosity gradients, and fluid disequilibrium. The EOS model shows that asphaltene concentration gradients can be large owing to both the gravity term and gas/oil ratio (GOR) gradients. The FHZ EOS is reduced to a very simple form—the gravity term only for low GOR black oils and heavy oils—and heavy oils are shown to exhibit enormous asphaltene concentration gradients in contrast to predictions from conventional models. In this paper, the FHZ EOS has been applied not only to calculate asphaltene concentration gradients but also to predict asphaltene phase instability in oil reservoirs. Two types of tar mats are discussed: one with a large discontinuous increase in asphaltene concentration versus depth typically at the base of an oil column (corresponding to asphaltene phase transition); the second with a continuous increase in asphaltene content at the base of a heavy oil column due to an exponential increase in viscosity with asphaltene content. Both types of tar mats are consistent with the Yen−Mullins model of asphaltenes within the FHZ EOS analysis discussed herein. The predictions are in good agreement with the laboratory and field observations, and the mechanisms of forming these two kinds of tar mats are also discussed. This methodology establishes a powerful new approach for conducting the analyses of asphaltene concentration grading and tar mat formation in oil reservoirs by integrating the Yen−Mullins model and the FHZ EOS with DFA technology.

■ INTRODUCTION

In a general sense, understanding asphaltene concentration distributions in reservoirs is broadly important due to the huge dependence of crude oil viscosity on asphaltene content. Asphaltene concentration distributions can also be useful for understanding reservoir architecture. In addition, immobile asphaltic layers or tar mats can be very detrimental to the production of oil because they generally preclude aquifer support in production and likewise preclude pressure support via water injection into the aquifer. Consequently, tar mats are of great importance in oil production. In the conventional terminology that is used worldwide in the oil business, one identifies two kinds of tar mats, typically but not always found at the base of an oil column. Nevertheless, the mechanisms of tar mat formation have long been a puzzle in the oil industry. For production of oil, these two types of tar mats are viewed as operationally identical. One kind of tar mat is defined as having a large and discontinuous increase in asphaltene content versus depth in the oil column. Frequently, in this case the oil is not very heavy. The development of this type of tar mat corresponds to a colloidal instability or a phase transition of asphaltenes. As a result, flow assurance problems are often encountered during production, especially in gas injection processes. The second kind of tar mat forms at the base of a heavy oil column. In this case, there can be a gravitational increase of asphaltene (clusters) toward the base of the column. Viscosity depends exponentially on asphaltene content; as the asphaltene content gets into tens of percent, the viscosity can become extremely high yielding a tar mat (immobile super heavy oil zone). There is considerable literature about tar mats and mechanisms were proposed to explain the formation of tar mats.[1−4] However, there have been no simple thermodynamic models available in the literature to explain the formation of tar mats. Herein, a simple physical model is introduced for the formation of both kinds of tar mats aiding in the understanding of critical issues in reservoirs.

Asphaltenes are defined as the fraction of petroleum soluble in toluene and insoluble in *n*-heptane. This definition largely captures that fraction of crude oil that self-assembles into nanoaggregates. As will be discussed, the nanoscience of asphaltenes in mobile crude oils has largely been worked out specifically yielding the gravity term and generally enabling development of equations of state (EOSs) for asphaltene concentration gradients. The Flory−Huggins−Zuo (FHZ) EOS is the first simple explicit EOS for predicting asphaltene

Received: August 10, 2011
Revised: January 26, 2012
Published: January 26, 2012

dx.doi.org/10.1021/ef201218m | *Energy Fuels* 2012, 26, 1670−1680

concentration gradients and as such is a critical development in petroleum science particularly as related to oil reservoirs. It builds on the existing Flory–Huggins EOS which has previously been used to model phase behavior of asphaltene precipitation.[5−9] Hirschberg[4] suggested the use of the Flory–Huggins regular solution model to describe asphaltene gradients—an idea that would prove to be very insightful. However, asphaltene dispersions in crude oil were not understood at that time, nor was there a thorough understanding of the solubility of asphaltenes in crude oils. As such, the original treatments ignored variations of fluid properties with depth such as gas/oil ratio and density gradients, which have been shown to play an important role for asphaltene concentration gradients. Moreover, the new, simple form of the FHZ EOS allows practical application of this model to oil reservoirs utilizing various measurements of reservoir fluid properties in particular by employing asphaltene concentration ratios or optical density ratios at two different depths in the reservoir as done in this paper. A dozen case studies have shown that the FHZ EOS can be applied to address major concerns in oil reservoirs through a new technology—downhole fluid analysis coupled with the FHZ EOS. Recently, Zuo et al.[10−14] and Freed et al.[15] developed a simple model with an explicit expression—the FHZ EOS—for analyzing equilibrium asphaltene concentration gradients to delineate reservoir connectivity by integrating the Yen–Mullins model[16] of asphaltenes and coupling with downhole fluid analysis measurements. This integrated approach has successfully been used to analyze reservoir connectivity for gas condensates, black oils, and heavy oils.[16−20] The subsequent production performance provided proof that the Yen–Mullins model, coupled with the FHZ EOS, DFA data, and asphaltene equilibration, successfully predicts connectivity in cases where classical cubic EOS models could not. For example, gas/oil ratios (GORs) are largely invariant in gas-lean highly undersaturated black oil columns, so GOR trends can not be used to infer grading or connectivity.[21]

In addition, the perturbed-chain statistical associating fluid theory (PC-SAFT) EOS has successfully modeled asphaltene phase behavior for flow assurance.[22,23] Most recently, Panuganti et al.[24] applied the PC-SAFT EOS for the first time to model the asphaltene distribution due to gravity in oil columns. The EOS accounts for the effect of compressibility on oil properties and the variation of asphaltene partial molar volume with depth. The PC-SAFT generated asphaltene grading shows very good agreement with the field data of two very different reservoirs (black and light oil). For a black oil reservoir, the PC-SAFT and FHZ EOS yielded similar results. For the light oil reservoir, after accurately modeling the asphaltene compositional grading in the upper part of the reservoir, the PC-SAFT EOS predicted a transition to a region of high asphaltene concentration at the depth that a tar mat was found in the lower part of the reservoir.[24]

It is noted that the Flory–Huggins model is widely consistent with the PC-SAFT EOS for asphaltene related phase behavior[5−9,22,23] and the FHZ EOS is congruent with the PC-SAFT EOS for modeling asphaltene gradients in black oil and light oil.[16−20,24] For light oil, the nanoscale description of whether asphaltenes are molecules or nanoaggregates is not so important because (1) the size difference between molecules and nanoaggregates is not so great on the basis of the Yen–Mullins model[16] and (2) the light oil GOR gradient drives the bulk of the heavy end gradient. The FHZ predicts asphaltene molecules in the light oil which is consistent with the Yen–Mullins model.[16] For low GOR black oils, nevertheless, asphaltene nanoaggregates are required, which is the basis of the PC-SAFT approach by the consensus. However, for heavy oils, the clusters within the FHZ EOS dominate the asphaltene gradients because clusters are much larger than nanoaggregates, which give large gravity effects, and the GOR gradients are almost nonexistent. Consequently, it is believed that all EOS including the PC-SAFT would need to explicitly account for clusters as done in the FHZ EOS to model the huge observed asphaltene concentration gradients for heavy oils (e.g., the asphaltene gradient is about 50× bigger than that in black oil columns). Compared with the PC-SAFT EOS which requires SARA (saturates, aromatics, resins, and asphaltenes) analysis, GOR, and oil and gas compositions, the FHZ EOS explicitly gives the ratio of asphaltene concentrations at two depths. The relative concentrations of asphaltenes can be obtained by measuring optical density (OD), that is, absorption of light. Thus, the ratio of asphaltenes can be obtained at two depths and analyzed using the FHZ EOS because all inputs can be related to DFA measurements downhole; therefore, it can be used in downhole real time analysis, in particular, the FHZ EOS is reduced to the simple Boltzmann equation (only gravity term) for oil with relatively low GOR.

In this paper, the FHZ EOS has been used not only to estimate asphaltene concentration gradients but also to conduct asphaltene phase instability analysis. Two categories of tar mat formation have been predicted by the FHZ EOS at the base of oil columns for real oilfield cases. The predictions are in good agreement with the laboratory and field observations. The mechanisms of forming these two kinds of tar mats are discussed, which resolve a long time puzzle in the oil industry regarding the formation of tar mats.

The Yen–Mullins Model of Asphaltenes. Over the past decade, much progress has been made in relation to all areas of asphaltene science.[25] In particular, the molecular and colloidal structure of asphaltenes has largely been resolved and is now codified in the Yen–Mullins model.[16] The Yen–Mullins model provides us with a foundation for understanding the dispersion of asphaltenes in crude oil and has been successfully applied to numerous field case studies.[17−20] In the Yen–Mullins model, asphaltenes are dispersed, suspended, or both in crude oils and in solvents in three forms: molecules, nanoaggregates, and clusters of nanoaggregates as depicted in Figure 1.

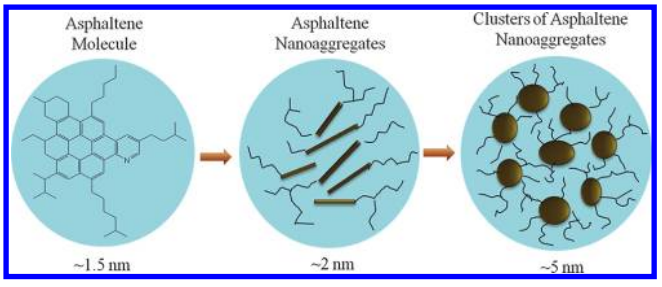

Figure 1. Yen–Mullins model, the new first principle paradigm of asphaltenes.[16] Asphaltene molecules have an average molar mass of ~750 g/mol and diameter of ~1.5 nm. Nanoaggregates have ~6 molecules, and clusters have ~8 nanoaggregates. Condensates have a molecular dispersion of heavy ends; stable black oils have asphaltenes in nanoaggregates, and unstable black oils and heavy oils have at least some asphaltenes in clusters of nanoaggregates.

dx.doi.org/10.1021/ef201218m | Energy Fuels 2012, 26, 1670–1680

Flory–Huggins–Zuo EOS for Asphaltene Concentration Gradients and Phase Instability. Because cubic equations of state are a variant of the van der Waals EOS which is derived from ideal gas law, they are not suited for asphaltene gradients. As we know, asphaltenes are colloidal solids and a cubic EOS has no provisions to handle such systems. Some researchers used cubic EOSs to deal with asphaltene precipitation in the literature. However, the critical properties and acentric factor of asphaltenes are usually estimated using the property correlations derived from relatively light pure hydrocarbons (typically up to C_{20}); molar mass is set to a value from hundreds to tens of thousands; and theses parameters are usually adjusted to match measured asphaltene precipitation data. As such, this is parametric and empirical. In contrast, the activity approach such as the Flory–Huggins regular solution model has been widely used in asphaltene precipitation modeling. Therefore, the activity approach is employed for asphaltene gradients in this work.

It is assumed that a reservoir fluid is treated as a mixture with two pseudocomponents: a solvent (nonasphaltene components or maltenes) and a solute (asphaltenes). The solvent is also a mixture whose properties are calculated by a cubic EOS as described in the Appendix; the details are given in refs 10–14 and 26–39. The mixture (bulk fluid–whole oil) properties are represented by no subscripts in the following expression. At constant temperature and pressure, the chemical potential of component i can be expressed as

$$(\mathrm{d}\mu_i)_{T,P} = (\rho\overline{v_i} - M_i)g\ \mathrm{d}h = \overline{v_i}\left(\rho - \frac{M_i}{\overline{v_i}}\right)g\ \mathrm{d}h \tag{1}$$

where μ_i, v_i, M_i, g, ρ, and h are the chemical potential, partial molar volume, and molar mass of component i, gravitational acceleration, density, and depth, respectively. It is further assumed that the partial molar volume of component i is equal to its molar volume, which is true for highly incompressible components such as asphaltenes. Therefore, $\rho_i = (M_i/v_i)$ is the density of component i. Thus, eq 1 can be rewritten as

$$(\mathrm{d}\mu_i)_{T,P} = \mathrm{d}(RT\ln x_i\gamma_i f_i^0) = v_i(\rho - \rho_i)g\ \mathrm{d}h \tag{2}$$

where f^0 is the fugacity at the reference state. R and T are the universal gas constant and temperature, respectively. The activity coefficient can be estimated by the multicomponent Flory–Huggins regular solution model

$$\ln\gamma_i = \ln\left(\frac{\phi_i}{x_i}\right) + 1 - \frac{v_i}{v} + \frac{v_i}{RT}(\delta_i - \delta)^2 \tag{3}$$

where ϕ and δ are the volume fraction and solubility parameter. The mixture parameters can be calculated by

$$v = \sum_i x_i v_i \qquad \text{and} \qquad \delta = \sum_i \phi_i\delta_i \tag{4}$$

Substituting eq 3 into eq 2 and integrating it at two depths (h_2 and h_1) if $\Delta h = h_2 - h_1$ is small enough and ignoring the fluid density difference between Δh, we obtain the Flory–Huggins–Zuo (FHZ) EOS for asphaltene concentration grading

$$\begin{aligned}\frac{\mathrm{OD}(h_2)}{\mathrm{OD}(h_1)} &= \frac{\phi_a(h_2)}{\phi_a(h_1)} \\ &= \exp\left\{\frac{v_a}{RT}[(\delta_a - \delta)_{h_1}{}^2 - (\delta_a - \delta)_{h_2}{}^2]\right\} \\ &\quad \times \exp\left\{\frac{v_a g(\rho - \rho_a)(h_2 - h_1)}{RT}\right\} \\ &\quad \times \exp\left\{v_a\left[\left(\frac{1}{v}\right)_{h_2} - \left(\frac{1}{v}\right)_{h_1}\right]\right\}\end{aligned} \tag{5}$$

where ϕ and δ are the volume fraction and solubility parameter, respectively. OD is the optical density measured by DFA,[21] which is linearly related to asphaltene content.[18,40] Subscript a denotes the properties of asphaltenes; subscripts h_1 and h_2 stand for the properties at depths (or heights) h_1 and h_2, respectively. The solubility parameter, molar volume, and density of bulk fluids are dependent on depth. Therefore, the concentration (volume fraction) variations of asphaltenes with depth depend on three terms: solubility (enthalpy), gravity, and entropy. It is noted that temperature also varies with depth. The details with regard to model parameters are given in ref 13.

Once the properties of oil and asphaltenes are obtained by the method described in the Appendix, the only adjustable parameter is the size (molar volume or diameter) of asphaltenes, which is determined by matching DFA measurements of optical density (asphaltene concentration) gradients. The obtained size is compared with the Yen–Mullins model[16] to check whether they are consistent. If not, then the fitted size of asphaltenes is not physically meaningful and cannot be used for reservoir connectivity and asphaltene phase instability. In other words, the size of asphaltenes can be assumed to be one of three asphaltene forms in the Yen–Mullins model (asphaltene molecules, nanoaggregates, or clusters) and then optical density (which correlates with asphaltene concentration) gradients can be predicted by the FHZ EOS by inference from asphaltenes. The asphaltene hard spherical diameter is typically within 15% uncertainties of these values based on 1.3 nm for asphaltene molecules, 1.8 nm for asphaltene nanoaggregates, and 5 nm for asphaltene clusters, respectively. In some cases, a combination of the colloidal and molecular asphaltenes can be present.

For a reservoir under active late gas charging and/or large thermal diffusion, the reservoir fluid is not equilibrated. To deal with such nonequilibrium oil column, the cubic EOS is first used to describe the nonequilibrium compositional gradient of the reservoir fluid. For example, when gas charges into an oil column, the gaseous charge quickly rises to the top of the reservoir through high mobility streaks, then the gas can diffuse slowly downward into the oil column. The cubic EOS coupled with a diffusion term can account for the composition versus depth. Then the FHZ EOS is used to calculate the asphaltene concentration gradient with the assumption of local asphaltenes equilibrated with a local fluid (local GOR and composition) at each small vertical depth interval. The asphaltene concentration gradient in the nonequilibrium hydrocarbon reservoir column is thus obtained, which can also be used for the analysis of reservoir connectivity and asphaltene phase instability.

dx.doi.org/10.1021/ef201218m | Energy Fuels 2012, 26, 1670–1680

After asphaltene concentrations are obtained at different depths, phase equilibrium calculations can be performed at all depths to check whether the asphaltenes can be stably dispersed or suspended in crude oils using the Flory–Huggins model which is also used for asphaltene concentration gradients in the FHZ EOS with the same set of parameters. If asphaltenes are unstable, then a first type of tar mat may form at that depth, which may result in formation damage and flow assurance problems during production. To conduct this analysis, the following equilibrium criteria must be satisfied for all components (asphaltene and maltene) at each depth

$$x_i^{\mathrm{oil}}\gamma_i^{\mathrm{oil}} = x_i^{\mathrm{asph}}\gamma_i^{\mathrm{asph}} \tag{6}$$

where superscripts oil and asph represent the oil-rich and asphaltene-rich phases and x is the mole fraction. Because the equilibrium criteria are used at the same depth for both phases, the gravitational term can be canceled out in the FHZ EOS. Therefore, the FHZ EOS is reduced to the Flory–Huggins regular solution model.

For heavy oil, if asphaltenes are stable but their content is as high as tens of percent, asphaltene clusters are formed based on the Yen–Mullins model and viscosity should be checked because viscosity increases exponentially with asphaltene content. Extremely high viscosity may yield immobile super heavy oil, and the second kind of tar mat may be formed at the base of a heavy oil column.

It is assumed that the density of asphaltenes is 1.2 g·cm^{-3}, and the solubility parameter of asphaltenes is estimated by the following relation

$$\delta_a(T) = \delta_a(T_0)[1 - 1.07 \times 10^{-3}(T - T_0)] \tag{7}$$

where T_0/K (= 298.15) is the reference temperature for solubility parameters of asphaltenes. $\delta(T_0)/(\mathrm{MPa})^{0.5}$ = 21.85.

RESULTS AND DISCUSSIONS

Asphaltene Instability Downhole. The first field case is a black oil column with GOR of about 125 m^3·m^{-3}.[16] This sandstone reservoir has temperature of about 120 °C. Geochemical analysis indicated that this crude oil has been gas washed.[41] A fraction of asphaltenes is destabilized by a late stage of gas charge. The asphaltene onset pressure was measured in a laboratory and is equal to the formation pressure, and asphaltene-rich hydrocarbons were found in the cores of the lower portion of this oil column.[41] A huge optical density gradient (thus asphaltene concentration gradient) was found: a gradient of a factor of 10 in about 80 m true vertical depth (TVD). The continuous pressure gradient data show that the oil zone is in pressure communication, which is a necessary condition but insufficient condition to establish flow connectivity.[21] The vertical interference test (VIT) data also show the oil column is connected.[41] The FHZ EOS was used to simulate this case for analysis of reservoir connectivity, asphaltene concentration grading, and asphaltene phase transition. The cubic EOS was used to calculate the oil compositional gradient. The FHZ EOS were used to estimate the asphaltene concentration gradient and then to predict asphaltene phase instability.

The cubic EOS[35] and the delumping and characterization methods proposed by Zuo et al.[37−39] were used to calculate compositional gradients for this black oil by solving eq A-10. Because the geochemical analysis indicated that this crude oil has been gas washed,[41] this oil column is very slightly nonequilibrium and external flux can be used. For simplicity, however, a small thermal gradient was used to compensate the impact of the external flux in the compositional gradient calculations using the cubic EOS. The calculated variations of molar volume, density, and solubility parameter with depth are shown in Figure 2. The oil column has some GOR gradient and density gradient with depth.

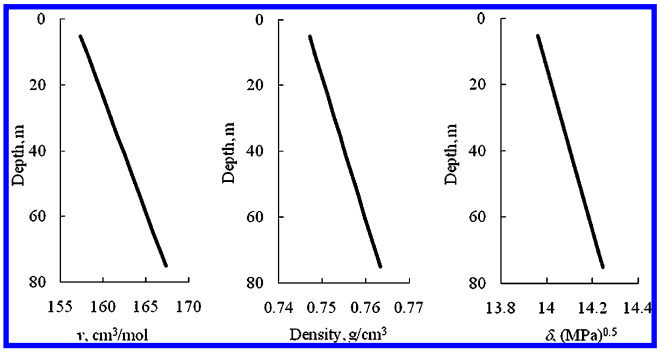

Figure 2. Variations of oil properties with depth calculated by the cubic EOS[35] for destabilized black oil.

The properties of bulk fluids shown in Figure 2 were used in the FHZ EOS. The only one underdetermined parameter in the FHZ EOS is the size of asphaltenes. As mentioned previously,[16] asphaltene nanoaggregates and clusters coexist in the black oil owing to asphaltene destabilization. The optical density analysis results are depicted in Figure 3. The dashed curve is computed

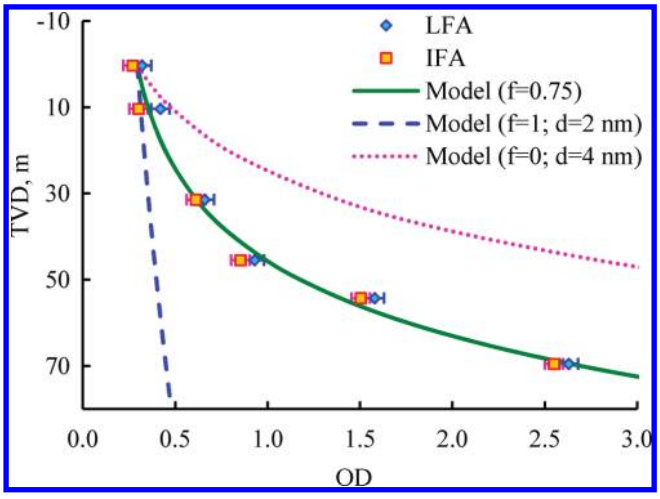

Figure 3. Huge asphaltene (optical density) gradient in a destabilized black oil column. The equilibrium asphaltene concentration distribution suggests that the oil zone is connected: (LFA) live fluid analyzer; (IFA) insitu fluid analyzer.

by the FHZ EOS with asphaltene nanoaggregates only, which is significantly underpredicts the asphaltene gradient. On the other hand, the dotted curve is calculated by the FHZ EOS with clusters of asphaltene nanoaggregates (4 nm in diameter), which significantly overestimates the asphaltene gradient. The field data are in good agreement with an equilibrium distribution of 75% asphaltene nanoaggregates +25% clusters. The equilibrium asphaltene concentration distribution indicates the oil zone is connected, which is consistent with the vertical interference test and continuous pressure gradient.[41]

dx.doi.org/10.1021/ef201218m | Energy Fuels 2012, 26, 1670−1680

The calculated asphaltene gradient is then used to analyze asphaltene phase instability at each depth using the FHZ EOS and the same parameters by solving eq 6. Figure 4 shows the

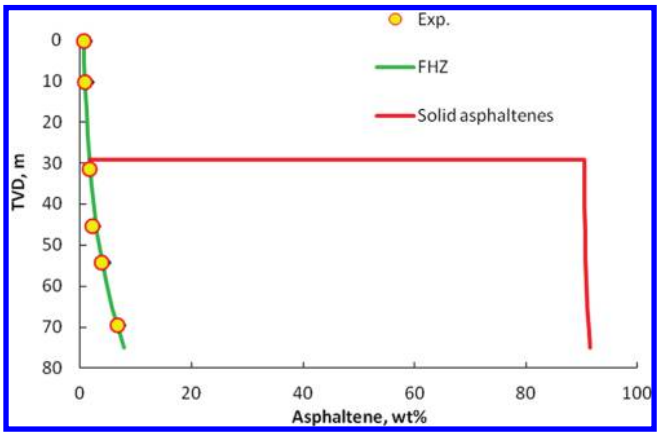

Figure 4. Asphaltenes phase instability at the base of the black oil column caused by a late stage of gas charge which is confirmed by geochemical analysis. The analysis was confirmed by the field evidence: (a) the asphaltene onset pressure was equal to the formation pressure and (b) asphaltene-rich hydrocarbons were found in the core.

asphaltene phase instability results predicted by the FHZ EOS. The FHZ EOS predicts that asphaltenes are unstable at the base of the oil column which is in agreement with the field and laboratory data as mentioned previously: (1) the asphaltene onset pressure was equal to the formation pressure at the depth where the FHZ EOS predicts asphaltene destabilization and (2) asphaltene-rich hydrocarbons were found in the cores of the lower portion of this oil column albeit in low quantities thereby not interfering with reservoir quality.[41] The clusters are formed from a fraction of asphaltene nanoaggregates because the late stage of gas charging (which is corroborated by a geochemistry analysis of volatile components) lowers the oil solvation power (solubility parameters) in the oil column and thus causes asphaltene destabilized. Depressurization may result in more destabilized and phase separated asphaltenes and reduction of porosity and permeability, as well as asphaltene blockages in the well bores during production.

Discrete Tar Mat: Discontinuous Asphaltene Concentration vs Depth. Excessive gas or condensate charge in the reservoir can destabilize the asphaltenes, thereby causing the first type of tar mat formation which is characterized by a *discontinuous* increase of asphaltene concentration with height in the hydrocarbon column. This happened in a reservoir initially filled with crude oil.[42] So much gas charged into the reservoir that the asphaltenes were destabilized to flocs *after* accumulating as clusters at the base of the oil column. Compositional and isotopic analysis of mud gas is displayed in Figure 5, which includes methane carbon isotope content and gas ratio (C_1/C_2). Both isotope and gas ratio analyses imply an increasing amount of thermogenic gas downdip or, conversely, an increasing amount of biogenic gas updip because two distinct processes produce hydrocarbon gas: biogenic and thermogenic degradation of organic matter. Biogenic gas is formed at shallow depths and low temperatures (<80 °C) by anaerobic bacterial decomposition of organic matter.[43,44] In contrast, thermogenic gas is formed at deeper depths by (1) thermal cracking of sedimentary organic matter into hydrocarbon liquids and gas (this gas is cogenetic with oil, and is called "primary" thermogenic gas) and (2) thermal cracking of oil at high temperatures into gas ("secondary" thermogenic gas) and pyrobitumen. Biogenic gas is very dry (i.e., it consists almost entirely of methane). In contrast, thermogenic gas can be dry, or can contain significant concentrations of "wet gas" components (ethane, propane, butanes) and condensate (C_{5+} hydrocarbons). This observation indicates that this condensate

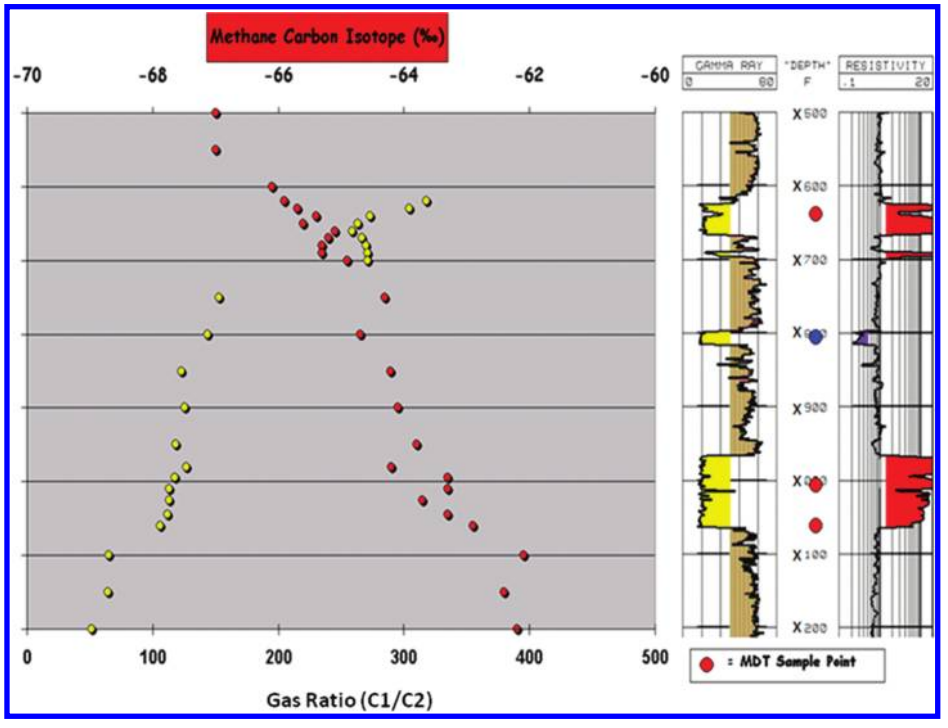

Figure 5. Methane $\delta^{13}C$ (red dots) and gas ratio (yellow dots) from mud gas logging in Well no. 1. The reservoir fluid is not equilibrated; biogenic methane is preferentially pooling updip in the reservoir.

dx.doi.org/10.1021/ef201218m | *Energy Fuels* 2012, 26, 1670–1680

gas column is not equilibrated. Even methane, the hydrocarbon component with the highest mobility, is not equilibrated.

Flow assurance issues were encountered in production streams in this field. Additionally, phase instability of asphaltenes for fluids in Well no. 1 is indicated in Figure 6.

Figure 6. Evidence of asphaltene destabilization is shown in this photograph. Commingled fluid from Well nos. 1 and 2 (left) and precipitated asphaltenes in Well no. 1 gas stream (right).

Fluids combined from Wells nos. 1 and 2 are shown in the picture to the left while globules precipitated from Well no. 1 gas stream are shown in the picture to the right. Figure 7 shows

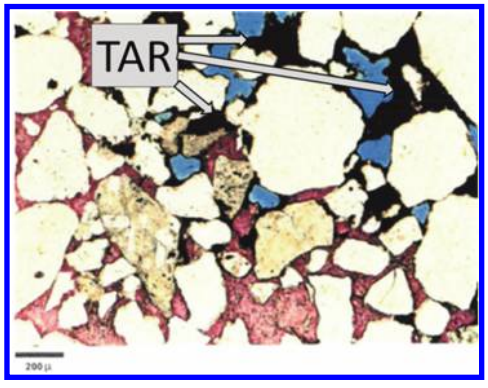

Figure 7. Thin section showing the presence of tar (black) just above the cemented (pink) section of the sandstone (white). The blue is pore space, not water. Water had no role on the formation of this tar mat.

the existence of tar resting just above cement in the permeable sections of core.

The cubic and FHZ EOS were used to simulate this hydrocarbon column for analysis of connectivity, asphaltene concentration gradients, and tar mat formation. First, the cubic EOS[35] was used to simulate the phase behavior of the reservoir fluid. Figure 8 compares compositional gradients between the laboratory data and the EOS results assuming that the external methane influx is 0.2 std $m^3 \cdot m^{-2} \cdot MY^{-1}$ in the downdip direction. The GOR and API gravity are compared in Figure 9. The EOS results are in good agreement with the measured data.

The FHZ EOS was then used to estimate the asphaltene and optical density gradients in this hydrocarbon column based on the results of the fluid property gradients calculated by the cubic EOS. The calculated asphaltene and optical density gradients are compared with the measured data in Figure 9. The obtained asphaltene diameter is 1.22 nm, which is consistent with asphaltene molecules in the Yen–Mullins

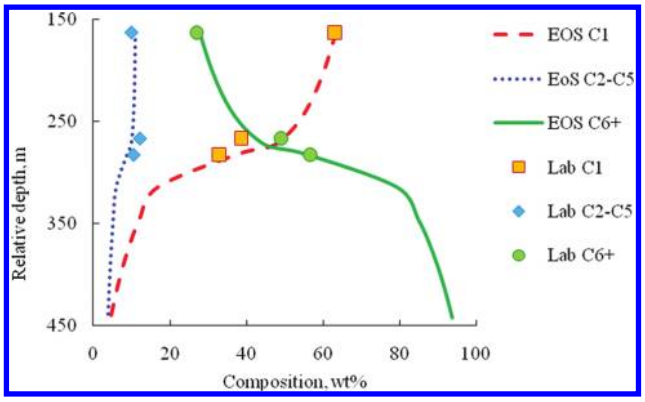

Figure 8. Nonequilibrium compositional gradients with depth calculated by the cubic EOS[35] with a methane influx in the downdip direction.

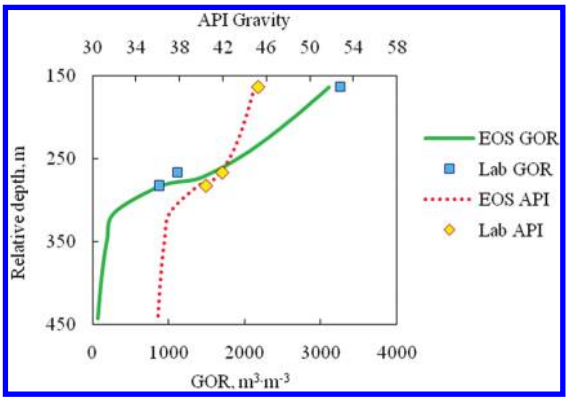

Figure 9. GOR and API gravity gradients with depth calculated by the cubic EOS[35] with a methane influx in the downdip direction.

model because the condensate gas which has very low solvation power for asphaltenes causes a very low concentration of asphaltenes molecularly dispersed in the condensate gas. The optical density analysis implies that the shallow DFA station is disconnected with the two deep DFA stations because all the data do not lie on the same theoretical curve.

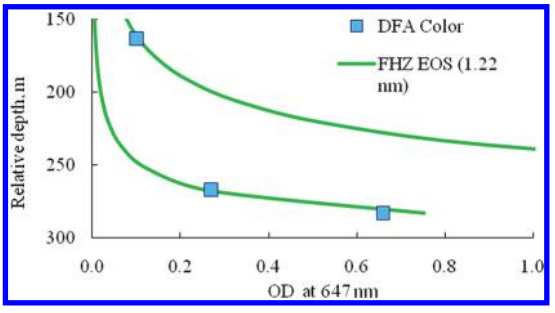

Figure 10. Optical density versus depth for a condensate gas column. The obtained asphaltene diameter is 1.22 nm, which is consistent with asphaltene molecules in the Yen–Mullins model. The optical density measurement at the short wavelength (647 nm) is consistent with low asphaltene concentration, thus the true molecular solution of asphaltenes.

The FHZ EOS was used to estimate the asphaltene concentration gradients by extending to the oil rim. Figure 10 shows the asphaltene gradient with depth estimated by the FHZ EOS. In the condensate gas, asphaltene concentration is

dx.doi.org/10.1021/ef201218m | Energy Fuels 2012, 26, 1670–1680

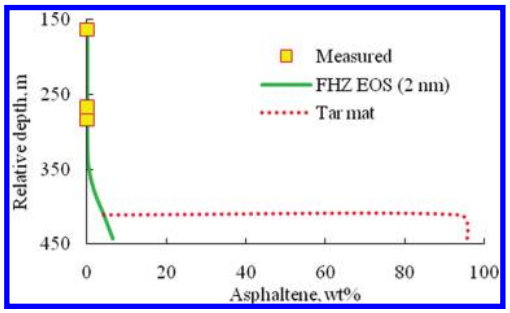

Figure 11. Asphaltene phase instability (tar mat formation) at the base of the gas condensate column caused by a late stage of gas charge which is confirmed by methane carbon isotope analysis.

nearly zero and the DFA measured optical densities at 1070 nm (linearly related to *n*-heptane asphaltenes) are zero as well. The asphaltene concentration gradient was then extended to the oil rim by the FHZ EOS and assuming a very small amount of asphaltenes at the gas/oil contact (GOC) and asphaltene diameter is 2 nm. It can be seen that asphaltenes are concentrated at the base of the oil rim. The estimated asphaltenes were checked by the FHZ EOS for phase instability (see Figure 11). It was found that the asphaltenes at the base of the oil column were destabilized to form a tar mat (a large and discontinuous increase in asphaltene content versus depth). The sensitivity analysis was conducted by changing asphaltene content at the GOC. The destabilized asphaltenes could be found at the base of oil column when asphaltene content reached greater than 4 wt % regardless the assumption of asphaltene content at the GOC.

The FHZ EOS results are in accord with the field and laboratory observations: (1) flow assurance issues encountered in production streams in this field as shown in Figure 6 and (2) the existence of tar in the permeable sections of core, of course not in the sections sealed by cement as shown in Figure 7. Clearly, cementation occurred first, and then, tar formed subsequently. The physical destabilization of asphaltenes in an oil column is often due to gas charge into a crude oil. The sequential mechanism proposed here for tar mat formation includes: (1) a late gas charge migrated into the reservoir moving to the top of the hydrocarbon column beneath the upper reservoir seal.[45] (2) The gas then diffused down into the oil column very slowly over geologic time, thus increasing GOR substantially near the top of the column. (3) This, in turn, reduced the solubility of asphaltenes at the top of the column causing the nanoaggregates adhere to each other forming colloidally stable clusters, (4) gravitational accumulation of the clusters toward the base of the column follows, and finally (5) asphaltenes concentrated at the base can exceed the solvency of the oil for asphaltenes yielding phase separation of solid asphaltenes to form a tar mat (cf Figure 7).

Continuous Tar Mat; Continuous Asphaltene Concentration vs Depth. For heavy oil with little compressibility, GOR is very small, and thus, a GOR gradient is likely negligible. However, because of the high concentration of asphaltenes, clusters of asphaltenes nanoaggregates can be stably suspended in heavy oil, and thus, a great asphaltene concentration gradient could be observed in the oil column even with a small maltene gradient.

In a field case,[16,20] the heavy oil with very low GOR of about 9 $m^3 \cdot m^{-3}$ has a significant asphaltene gradient (10 to 20 wt %) in about 20 m TVD. API gravity varies from 21 to 13 °API. The sandstone reservoir has temperature of about 93 °C, which is higher than the maximum biodegradation temperature (<80 °C).[43,44] This is nonbiodegraded heavy oil. The corresponding viscosity gradient is about a factor of 30 in 20 m TVD from 6 to 200 cP measured in the laboratory; hence, this gradient is extremely important for production. Note that in the relevant sand, the pressure gradient is continuous and production is resulting in pressure depletion throughout the heavy oil column indicating connectivity. The FHZ EOS was utilized to analyze the asphaltene gradient in this heavy oil column.

The FHZ EOS is reduced to a very simple form—the gravity term only for low GOR black oils and mobile heavy oils because the solubility and entropy terms have opposite contributions to asphaltene gradients and they are approximately canceled out. Heavy oils are shown to exhibit enormous asphaltene concentration gradients in contrast to predictions from conventional models. For instance, the asphaltene concentration increases by a factor of 2 in about 20 m TVD in this heavy oil column whereas that varies by a factor of 2 in about 1000 m TVD in the conventional low GOR black oil column for the Tahiti case[18] as shown in Figure 12 for sand M21B. The gradient in the mobile heavy oil is as about

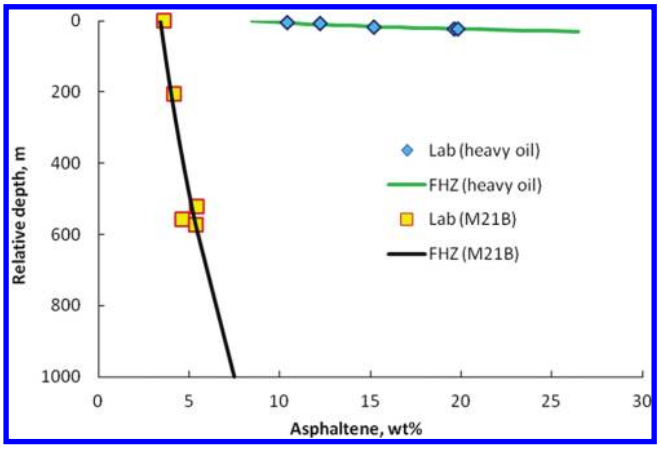

Figure 12. Comparison of asphaltene gradients in a heavy oil (clusters) and a low GOR black oil (nanoaggregates). The asphaltene gradient is about 50× vertically in the heavy oil in contrast to that in the low GOR black oil. The simplified FHZ EOS gravity term alone also gives the asphaltene gradient of about 50× over the low GOR black oil.

50× that in the low GOR black oil. The curves in Figure 12 are calculated by the simplified FHZ EOS—the gravity term alone. Asphaltenes are present as nanoaggregates in the black oil and as clusters in the heavy oil.

Figure 13 shows the asphaltene variation with depth for the heavy oil. Using the full FHZ EOS, the fitted asphaltene diameter is 4.7 nm, which is consistent with asphaltene clusters in the Yen–Mullins model. The equilibrium distribution of clusters of asphaltene nanoaggregates indicates that the oil zone is connected, which is in accord with the pressure depletion.

The estimated asphaltene gradients were used to conduct asphaltene phase instability analysis by solving eq 6. The analysis suggests there are no destabilized asphaltenes in the oil column. In spite of high asphaltene concentration and a large

dx.doi.org/10.1021/ef201218m | *Energy Fuels* 2012, 26, 1670–1680

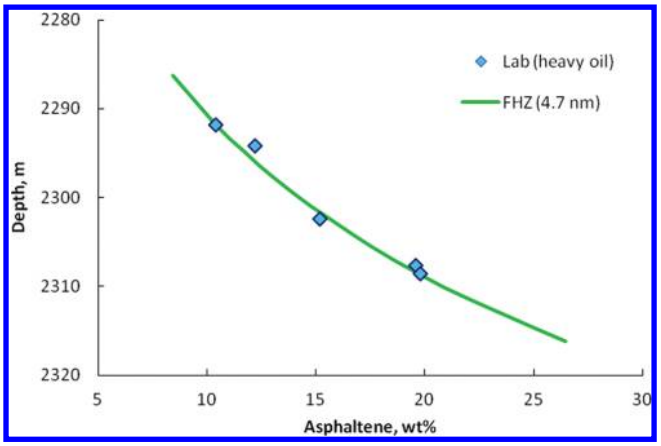

Figure 13. Significant asphaltene gradient in a heavy oil column. The asphaltene gradient is in accord with an equilibrium distribution of clusters of asphaltene nanoaggregates with spherical diameter of 4.7 nm. The continuous equilibrium distribution implies the formation connectivity, which is consistent with but not proven by the continuous pressure gradient.

gradient, clusters of asphaltene nanoaggregates can be stably suspended in heavy oil because maltenes in heavy oil have high solubility parameters (high solvation power) and very low concentration of dissolved gas (GOR) to keep asphaltenes stable in mobile heavy oil columns. To conduct sensitivity analysis, the solubility parameters of bulk heavy oil were significantly decreased but no unstable asphaltenes were found. For nonbiodegraded heavy oil, a continuous-type tar mat can form at its base. Here, one possible mechanism is presented for formation of an immobile super heavy oil zone (also referred to as a tar mat by oil operating companies); other mechanisms might work as well.

Let us look at viscosity in this heavy oil column. The Pal–Rhodes model[46] and the Mooney model[47] were modified to calculate viscosity for stock tank heavy oil in the open literature.[48,49] If viscosity at a reference (η_0) is known, the modified Pal–Rhodes model can be used to calculate viscosity for stock tank heavy oil

$$\frac{\eta}{\eta_0} = \left[\frac{1 - K'A}{1 - K'A_0}\right]^{-\nu} \tag{8}$$

The subscript 0 denotes the properties at the reference condition. Lin et al.[48] found $\nu = 6.9$ for heavy oil. K' is treated as an adjustable parameter in this paper. A is the mass fraction of asphaltenes in stock tank oil.

The modified Mooney model[49] is given by

$$\frac{\eta}{\eta_0} = \exp\left[[\eta]\left(\frac{A}{1 - \frac{A}{A_{max}}} - \frac{A_0}{1 - \frac{A_0}{A_{max}}}\right)\right] \tag{9}$$

It is assumed $A_{max} = 0.7$,[49] and $[\eta]$ is treated as an adjustable parameter in this paper. The modified Pal–Rhodes and Mooney models were validated by adding precipitated asphaltenes to deasphalted heavy oil at different asphaltene content and temperature, with viscosity up to 50 000 cP.[49]

For live heavy oil, the effects of GOR, pressure, and temperature on viscosity are considered by the following proposed expression

$$\left(\frac{\eta}{\eta_0}\right)_{live} = \left(\frac{\eta}{\eta_0}\right)_{STO}\left[\left(\frac{R_{s0}}{R_s}\right)^{1/3}\right]\left(\frac{T_0}{T}\right)^{4.5} \times \exp[1.392 \times 10^{-2}(p - p_0)] \tag{10}$$

Pressure (p in megapascals), temperature (T in kelvin), and GOR (R_s in cubic meters per cubic meter) corrections are similar to the expressions given by Khan[50] for undersaturated oil where viscosity is inversely proportional to $R_s^{1/3}$ and $T^{4.5}$.

The correlated viscosity results for this live heavy oil at reservoir conditions are shown in Figure 14. $K' = 2.65$, and

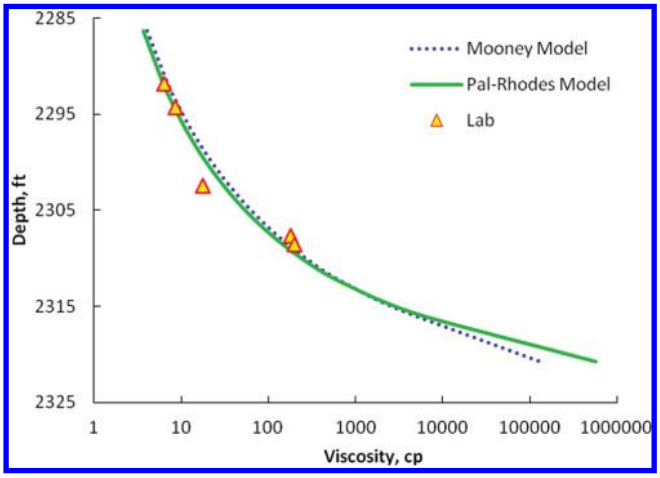

Figure 14. Significant viscosity gradient in a heavy oil column. A continuous asphaltene gradient with depth results in an exponential increase of heavy oil viscosity. High viscosity heavy oil leads to an immobile tar mat at the base of the heavy oil column.

$[\eta] = 19$. The correlated results are in good agreement with the measured data.

It can be seen that viscosity increases significantly at the base of the heavy oil column. For instance, viscosity rises from 2324 cP at 2314 m (mobile oil) to more than 130 000 cP at 2320 m (immobile super heavy oil or tar) predicted by the models. It should be noticed that the viscosity model has been validated for heavy oil up to 50 000 cP. Therefore, the second type of tar mat can form at the base of a heavy oil column simply by a gravitationally induced continuous increase of asphaltene content in the heavy oil column over geologic time leading to a huge viscosity at the base of the column. Of course, the other kind of tar mat (asphaltene phase instability) is possible for heavy oil as well. It is important to note that biodegradation can also produce a continuous-type tar mat as well.[51] We do not treat this type herein, but note that biodegradation preferentially removes alkane doing two things: (1) the asphaltenes become concentrated at and near the oil–water contact (where the microbes are potentially active) and (2) the liquid phase of the oil becomes increasing a better solvent for asphaltenes as the alkanes are removed. This process can lead to large disequilibrium, continuous gradients of asphaltenes with very large viscosity at the base of the oil column.

Akkurt et al.[52] presented a mobile heavy oil column with 4 DFA stations where the heavy oil viscosities increase

dx.doi.org/10.1021/ef201218m | Energy Fuels 2012, 26, 1670–1680

exponentially from 8.7 to 1360 cP downward in a 15-m true vertical depth interval (mobility from 70 to 1.5 md·cp^{-1}). Below the mobile heavy oil column, there is a very thick immobile tar (tar mat). The FHZ EOS and the viscosity model were able to describe this oil column in a good agreement with the laboratory measurements, and the results will be published in a separate technical paper.

CONCLUSIONS

A simple model—the FHZ EOS combined with the Yen–Mullins model of asphaltene nanoscience—has successfully been used to conduct asphaltene concentration gradient and phase instability analyses in oil reservoirs. The FHZ model with emphasis on asphaltene clusters predicts the possible formation of a continuous-type tar mat at the base of heavy oil columns. In addition, the FHZ EOS accounts for discrete tar mat formation at the base of lighter oil columns via a gas charge process in reservoirs. The predictions are in good agreement with the laboratory and field observations. This methodology establishes a powerful new approach for conducting asphaltene concentration grading and tar mat formation analyses by integrating the Yen–Mullins model, and the FHZ EOS with DFA technology to address reservoir and fluid complexities.

APPENDIX

Equations of Compositional Gradients

Since the 1980s, many researchers have worked on modeling of compositional grading in reservoir columns using equations of state (EOS).[11,26−32] For a mixture of reservoir fluids with N-components, a set of mass flux equations for all components are expressed as

$$J_i = J_i^{\mathrm{Chem}} + J_i^{\mathrm{Gr}} + J_i^{\mathrm{Therm}} + J_i^{\mathrm{Press}} \qquad i = 1, 2, ..., N \tag{A-1}$$

where J_i is the mass flux of component i. The superscripts Chem, Gr, Therm, and Press stand for the fluxes due to chemical, gravitational, thermal, and pressure forces, respectively.

To calculate compositional gradients with depth in a hydrocarbon reservoir using EOS, it is usually assumed that all the components of reservoir fluids have zero mass flux, which is a stationary state in the absence of convection.[26,27] At the stationary state, the fluxes in eq A-1 are equal to the external flux at the boundary of the system. The external flux could be an active gas charge, J_i^{e}. For simplicity, it is assumed that the external mass flux is constant over the characteristic time scale of the filling mechanisms in the formation.[28−30] By taking into account the driving forces due to chemical, gravitational, pressure, thermal impact, and external flux, the resulting equations are given by

$$\sum_{j=1}^{N}\left(\frac{\partial \mu_i}{\partial x_j}\right)_{T,P,n_{j\neq i}} \nabla x_j - (M_i - \overline{v}_i\rho)g + \frac{F_{Ti}}{T}\nabla T + \frac{J_i^{\mathrm{e}}RT}{x_i\rho D_i} = 0, \qquad i = 1, 2, ..., N \tag{A-2}$$

where μ_i, x_i, v_i, M_i, D_i, g, R, ρ, and T are the chemical potential, mole fraction, partial molar volume, molar mass, and effective diffusion coefficient of component i, gravitational acceleration, universal gas constant, density, and temperature, respectively. F_{Ti} is the thermal diffusion flux of component i. Since the chemical potential is a function of pressure, temperature, and mole fraction, it can be expressed under isothermal conditions as follows

$$(\nabla \mu_i)_T = \left(\frac{\partial \mu_i}{\partial P}\right)_{T,n} \nabla P + \sum_{j=1}^{N}\left(\frac{\partial \mu_i}{\partial x_j}\right)_{T,P,n_{j\neq i}} \nabla x_j \tag{A-3}$$

It is also assumed that the reservoir is in hydrostatic equilibrium, i.e.:

$$\nabla P = \rho g \tag{A-4}$$

According to the thermodynamic relations, the partial molar volume is defined as

$$\overline{v}_i = \left(\frac{\partial \mu_i}{\partial P}\right)_{T,n} \tag{A-5}$$

Therefore, the chemical potential change at constant temperature is rewritten as

$$(\nabla \mu_i)_T = \overline{v}_i\rho g + \sum_{j=1}^{N}\left(\frac{\partial \mu_i}{\partial x_j}\right)_{T,P,n_{j\neq i}} \nabla x_j = \overline{v}_i\rho g + (\nabla \mu_i)_{T,P} \tag{A-6}$$

Substituting eq A-6 into eq A-2, the following equation can be obtained:

$$(\nabla \mu_i)_T - M_i g + \frac{F_{Ti}}{T}\nabla T + \frac{J_i^{e}RT}{x_i\rho D_i} = 0, \qquad i = 1, 2, ..., N \tag{A-7}$$

The thermal diffusion flux of component i (F_{Ti}) can be calculated by the different thermal diffusion models. An example is the Haase expression[31,33]

$$F_{Ti} = M_i\left(\frac{H_\mu}{M_{\mathrm{m}}} - \frac{H_i}{M_i}\right) \tag{A-8}$$

where subscripts m and i stand for the property of the mixture and component i, respectively. H is the molar enthalpy. The chemical potential is calculated through the calculation of fugacity. The resulting equation in one vertical dimension is given by

$$\Delta(\ln f_i) - \frac{M_i g\Delta h}{RT} + M_i\left(\frac{H_{\mathrm{m}}}{M_{\mathrm{m}}} - \frac{H_i}{M_i}\right)\frac{\Delta T}{RT^2} + \frac{J_i^{e}\Delta h}{x_i\rho D_i} = 0, \qquad i = 1, 2, ..., N \tag{A-9}$$

where f_i is the fugacity of component i and h stands for the vertical depth. A cubic EOS such as the Peng–Robinson EOS[34,35] with volume translation[36] can be used to estimate the fugacity of component i. Therefore, eq A-9 is rearranged as

$$\ln(\varphi_i z_i P)|_h - \ln(\varphi_i z_i P)|_{h_0} = \frac{M_i g\Delta h}{RT} - M_i\left(\frac{H_{\mathrm{m}}}{M_{\mathrm{m}}} - \frac{H_i}{M_i}\right)\times\frac{(T - T_0)}{RT^2} - \frac{J_i^{\mathrm{e}}\Delta h}{x_i\rho D_i}, \qquad i = 1, 2, ..., N \tag{A-10}$$

where φ_i and z_i are the fugacity coefficient and mole fraction of component i, respectively, and h_0 denotes the reference depth.

dx.doi.org/10.1021/ef201218m | Energy Fuels 2012, 26, 1670−1680

The critical properties and acentric factors of components are required for the EOS to calculate fugacity coefficients. The delumping and characterization procedure of Zuo and Zhang[37] and Zuo et al.[38] is applied to characterize single carbon number and plus fractions of reservoir fluids at the reference depth, and the cubic EOS[35] is used to estimate fugacity. The DFA and/or PVT data are matched by tuning the EOS parameters and/or external gas charging flux to establish a reliable fluid EOS model. The compositions at depth h are thus obtained by solving eq A-10 numerically.

AUTHOR INFORMATION

Corresponding Author

*E-mail: yzuo@slb.com.

Notes

The authors declare no competing financial interest.

REFERENCES

(1) Mueller, III., H. W. General Model for Delivery of Asphaltenes to Tar Mats. *Presented at AAPG Annual Convention and Exhibition*, Houston, Texas, USA, April 10−13, 2011; Paper 40740.

(2) Masterson, IV., W. D. *Petroleum Filling History of Central Alaskan North Slope Fields*. PhD Dissertation, University of Texas at Dallas, 2001.

(3) Wilhelms, A.; Larter, S. R. Origin of Tar Mats in Petroleum Reservoirs. Part II: Formation Mechanisms for Tar Mats. *Mar. Pet. Geo L.* **1994**, *11*, 442−456.

(4) Hirschberg, A. Role of Asphaltenes in Compositional Grading of a Reservoir's Fluid Column. *J. Pet. Tech.* **1988**, No. January, 89−94.

(5) Buckley, J. S.; Wang, X.; Creek, J. L. Solubility of the Least Soluble Asphaltenes. In *Asphaltenes, Heavy Oils and Petroleomics*; Mullins, O. C., Sheu, E. Y., Hammami, A., Marshall, A. G., Eds.; Springer: New York, 2007; Ch. 16, pp 401− 438.

(6) Wang, J. X.; Buckley, J. S. A Two-Component Model of the Onset of Asphaltene Flocculation in Crude Oils. *Energy Fuels* **2001**, *15*, 1004−1012.

(7) Wang, J. X.; Creek, J. L.; Buckley, J. S. Screening for Potential Asphaltene Problems. *Presented at the 2006 SPE Annual Technical Conferences and Exhibition*, San Antonio, TX, USA, Sept 24−27, 2006; Paper SPE no. 103137.

(8) Creek, J. L.; Wang, J.; Buckley, J. S. Verification of Asphaltene-Instability-Trend (ASIST) Predictions for Low-Molecular-Weight Alkanes. *SPE Production Oper.* **2009**, *5*, 360−367.

(9) Vargas, F. M.; Gonzalez, D. L; Creek, J. L.; Wang, J. X.; Buckley, J.; Hirasaki, G. J.; Chapman, W. G. Development of a General Method for Modeling Asphaltene Stability. *Energy Fuels* **2009**, *23*, 1147−1154.

(10) Zuo, J. Y.; Mullins, O. C.; Dong, C.; Betancourt, S. S.; Dubost, F. X.; O'Keeffe, M.; Zhang, D. Investigation of Formation Connectivity Using Asphaltene Gradient Log Predictions Coupled with Downhole Fluid Analysis. *Presented at the SPE Annual Technical Conference and Exhibition*, New Orleans, Louisiana, Oct 4−7, 2009; Paper SPE 124264.

(11) Zuo, J. Y.; Mullins, O. C.; Dong, C.; Zhang, D.; O'Keefe, M.; Dubost, F.; Betancourt, S. S.; Gao, J. Integration of Fluid Log Predictions and Downhole Fluid Analysis. *Presented at the SPE Asia Pacific Oil and Gas Conference and Exhibition*, Jakarta, Indonesia, Aug 4−6, 2009; Paper SPE 122562.

(12) Zuo, J. Y.; Freed, D.; Mullins, O. C.; Zhang, D.; Gisolf, A. Interpretation of DFA Color Gradients in Oil Columns Using the Flory-Huggins Solubility Model. *Presented at the CPS/SPE International Oil & Gas Conference and Exhibition in China*, Beijing, China, June 8−10, 2010; Paper SPE 130305.

(13) Zuo, J. Y.; Freed, D.; Mullins, O. C.; Zhang, D. DFA Profiling of Oil Columns with Asphaltene Gradients. *Presented at the SPE Annual Technical Conference and Exhibition held in Florence*, Italy, Sep 19−22, 2010; Paper SPE 133656.

(14) Zuo, J. Y.; Mullins, O. C.; Freed, D.; Zhang, D. A Simple Relation between Densities and Solubility Parameters for Live Reservoir Fluids. *J. Chem. Eng. Data* **2010**, *55* (9), 2964−2969.

(15) Freed, D. E.; Mullins, O. C.; Zuo, J. Y. Theoretical Treatment of Asphaltenes in the Presence of GOR Gradients. *Energy Fuels* **2010**, *24* (7), 3942−3949.

(16) Mullins, O. C. The Modified Yen Model. *Energy Fuels* **2010**, *24* (4), 2179−2207.

(17) Gisolf, A.; Dubost, F. X.; Zuo, Y. J.; Williams, S.; Kristoffersen, J.; Achourov, V.; Bisarah, A.; Mullins, O. C. Real Time Integration of Reservoir Modeling and Formation Testing. *Presented at the EUROPEC/EAGE Annual Conference and Exhibition*, Amsterdam, June 8−11, 2009; Paper SPE 121275.

(18) Betancourt, S. S.; Dubost, F. X.; Mullins, O. C.; Cribbs, M. E.; Creek, J. L.; Mathews, S. G. Predicting Downhole Fluid Analysis Logs to Investigate Reservoir Connectivity. *Presented at IPTC*, Dubai, UAE, Dec 4−6, 2007; Paper SPE IPTC 11488.

(19) Betancourt, S. S.; Ventura, G. T.; Pomerantz, A. E.; Viloria, O.; Dubost, F. X.; Zuo, J.; Monson, G.; Bustamante, D.; Purcell, J. M.; Nelson, R. K.; Rodgers, R. P.; Reddy, C. M.; Marshall, A. G.; Mullins, O. C. Nanoaggregates of Asphaltenes in a Reservoir Crude Oil and Reservoir Connectivity. *Energy Fuels* **2009**, *23*, 1178−1188.

(20) Pastor, W.; Garcia, G.; Zuo, J. Y.; Hulme, R.; Goddyn, X.; Mullins, O. C. 2011 Measurement and EoS Modeling of Large Compositional Gradients in Heavy Oils. *Submitted to 53rd SPWLA Annual Symposium*, Cartagena, Colombia, June 16−20, 2012.

(21) Mullins, O. C. *The Physical of Reservoir Fluids: Discovery through Downhole Fluid Analysis*, Schlumberger: Sugar Land, Texas, USA, 2008.

(22) Vargas, F. M.; Gonzalez, D. L.; Hirasaki, G. J.; Chapman, W. G. Modeling Asphaltene Phase Behavior in Crude Oil Systems Using the Perturbed Chain Form of the Statistical Associating Fluid Theory (PC-SAFT) Equation of State. *Energy Fuels* **2009**, *23*, 1140−1146.

(23) Gonzalez, D. L.; Vargas, F. M.; Chapman, W. G.; Hirasaki, G. J. Modeling study of CO2-induced asphaltene precipitation. *Energy Fuels* **2008**, *22*, 757−762.

(24) Panuganti, S. R.; Vargas, F. M.; Chapman, W. G. Modeling of Reservoir Connectivity and Tar-Mat Using Gravity-Induced Asphaltene Compositional Grading. *Energy Fuels* **2011**, DOI: 10.1021/ef201280d.

(25) Mullins, O. C., Sheu, E. Y., Hammami, A., Marshall, A. G. Eds. *Asphaltenes, Heavy Oils and Petroleomics*; Springer: New York, 2007.

(26) Høier, L. *Miscibility Variations in Compositionally Grading Petroleum Reservoirs*. PhD thesis, Norwegian U. of Science and Technology, Trondheim, Norway, 1997.

(27) Høier, L.; Whitson, C. H. Compositional Grading−Theory and Practice. *SPE Reser. Eval. Eng.* **2001**, No. December, 525−535.

(28) Montel, F.; Bickert, J.; Caillet, G.; Le Goff, C. Modeling the Effect of External Gas Flux on Reservoir Fluid Description. *Presented at SPE Annual TCE*, San Antonio, Texas, Sept 29−Oct 2, 2002; Paper SPE 77383.

(29) Montel, F.; Bickert, J.; Hy-Billiot, J.; Royer, M. Pressure and Compositional Gradients in Reservoirs. *Presented at the SPE International Technical Conference and Exhibition*, Abuja, Nigeria, Aug 4−6, 2003; Paper SPE 85668.

(30) Montel, F.; Bickert, J.; Lagisquet, A.; Galliero, G. Initial State of Petroleum Reservoirs: A Comprehensive Approach. *J. Pet. Sci. Eng.* **2007**, *58*, 391−402.

(31) Pedersen, K. S; Lindeloff, N. Simulations of Compositional Gradients in Hydrocarbon Reservoirs under the Influence of a Temperature Gradient. *Presented at the SPE Annual Technical Conference and Exhibition*, Denver, Colorado, Oct 5−8, 2003; Paper SPE 84364.

(32) Creek, J. L.; Schrader, M. L. East Painter Reservoir: An Example of a Compositional Gradient from a Gravitational Field. *Presented at the 60th SPE Annual Technical Conference and Exhibition*, Las Vegas, NV, Sept 22−25, 1985; SPE Paper 14411.

(33) Haase, R.; Borgmann, H.-W.; Ducker, K. H.; Lee, W. P. Thermodiffusion im Kritischen Verdampfungsgebiet Binarer Systeme. *Naturforch* **1971**, *26a*, 1224−1227.

(34) Peng, D.-Y.; Robinson, D. B. A New Two-Constant Equation of State. *Ind. Eng. Chem. Fundam.* **1976**, *15*, 59−64.
(35) Peng, D.-Y.; Robinson, D. B. The Characterization of the Heptanes and Heavier Fractions for the PGA Peng-Robinson Programs. *GPA Research Report RR-28*, 1978.
(36) Peneloux, A.; Rauzy, E.; Freze, R. A Consistent Correction for Redlich-Kwong-Soave Volumes. *Fluid Phase Equilib.* **1982**, *8*, 7−23.
(37) Zuo, J. Y.; Zhang, D. Plus Fraction Characterization and PVT Data Regression for Reservoir Fluids near Critical Conditions. *Presented at the SPE Asia Pacific Oil and Gas Conference and Exhibition*, Brisbane, Australia, Oct 16−18, 2000; Paper SPE 64520.
(38) Zuo, J. Y.; Zhang, D; Dubost, F.; Dong, C.; Mullins, O. C.; O'Keefe, M.; Betancourt, S. S. EOS-Based Downhole Fluid Characterization. *SPE J.* **2011**, *16* (1), 115−124.
(39) Zuo, J. Y.; Mullins, O. C.; Freed, D.; Zhang, D.; Dong, C.; Zeng, H. Analysis of Downhole Asphaltene Gradients in Oil Reservoirs with a New Bimodal Asphaltene Distribution Function. *J. Chem. Eng. Data* **2011**, *56* (4), 1047−1058.
(40) Ruiz-Morales, Y.; Wu, X.; Mullins, O. C. Electronic Absorption Edge of Crude Oils and Asphaltenes Analyzed by Molecular Orbital Calculations with Optical Spectroscopy. *Energy Fuels* **2007**, *21* (2), 944−952.
(41) Mishra, V.; Hammou, N.; Skinner, C.; MacDonald, D.; Lehne, E.; Wu, J.; Zuo, J. Y.; Dong, C.; Mullins, O. C. *Downhole Fluid Analysis & Asphaltene Nanoscience coupled with VIT for Risk Reduction in Black Oil Production*, submitted to SPE, 2011.
(42) Elshahawi, H.; Latifzai, A. S.; Dong, C.; Zuo, J. Y.; Mullins, O. C. Understanding Reservoir Architecture Using Downhole Fluid Analysis and Asphaltene Science. *Presented at the 52nd SPWLA Annual Symposium*, Colorado Springs, May 14−18, 2011.
(43) Connan, J. Biodegradation of Crude Oils in Reservoirs. In *Advances in Petroleum Geochemistry*; Brooks, J., Welte, D. H., Eds.; Academic Press: London, 1984; Vol. *1*, pp 299−335.
(44) Barnard, P. C.; Bastow, M. A. Hydrocarbon Generation, Migration, Alteration, Entrapment and Mixing in the Central and Northern North Sea. In *Petroleum Migration*; England, W. A., Fleet, A. J., Eds.; Geological Society: London, 1991; pp 167−190, Special Publications.
(45) Stainforth, J. G. New Insights into Reservoir Filling and Mixing Processes. In *Understanding Petroleum Reservoirs: Towards an Integrated Reservoir Engineering and Geochemical Approach*, Cubitt, J. M., England, W. A., Larter, S. R., Eds.; Geological Society: London, 2004; pp 115−132, Special Publications 237.
(46) Pal, R.; Rhodes, E. Viscosity/concentration relationships for emulsions. *J. Rheol.* **1989**, *33*, 1021−1045.
(47) Mooney, M. The viscosity of a concentrated suspension of spherical particles. *J. Colloid Sci.* **1951**, *6*, 162−170.
(48) Lin, M. S.; Lunsford, K. M.; Llover, C. J.; Davison, R. R.; Bullin, J. A. The Effects of Asphaltenes on the Chemical and Physical Characteristics of Asphalt. In *Asphaltenes: fundamentals and applications*; Shu, E. Y., Mullins, O. C., Eds.; Plenum Press: New York, 1995; pp 155−176.
(49) Luo, P.; Gu, Y. Effects of asphaltene content on the heavy oil viscosity at different temperature. *Fuel* **2006**, *86*, 1069−1078.
(50) Khan, S. A.; Al-Marhoun, M. A.; Duffuaa, S. O.; Abu-Khamsin, S. A. Viscosity Correlations for Saudi Arabian Crude Oils. *Presented at the Fifth SPE Middle East Conference*, Manama, Bahrain, Mar 7−10, 1987; SPE Paper 15720.
(51) Larter, S.; Aplin, A. Mechanism of Petroleum Biodegradation and of Caprock Failure: New Insights, Applications of Reservoir Geochemistry. *Conference Abstracts: Geochemistry of Reservoirs II: Linking Reservoir Engineering and Geochemical Models*, Feb 3−4; Cubbitt, J., England, W., Larter, S., Macleod, G., Eds.; Geological Society of London, 2003.
(52) Akkurt, R.; Seifert, D.; Neumann, P.; Zeybek, M.; Hazim, A. In-Situ Heavy Oil Fluid Density and Viscosity Determination Using Wireline Formation Testers in Carbonates Drilled with Water-Based Mud. *Presented at 2010 Annual Technical Conference and Exhibition*, Florence, Italy, Sep 19−22, 2010; SPE Paper 134849.